AGU PUBLICATIONS

JGR

Journal of Geophysical Research: Biogeosciences

RESEARCH ARTICLE
10.1002/2015JG002939

Special Section:
Carbon and Nitrogen Fluxes at the Land-Ocean Interface

Key Points:
- Air-sea CO_2 fluxes are simulated using coupled biogeochemical-circulation model
- Shelf air-sea CO_2 fluxes respond differently to variable atmospheric forcing
- Temperature is very important in regulating air-sea CO_2 flux variability

Correspondence to:
B. Cahill,
cahill@informus.de

Citation:
Cahill, B., J. Wilkin, K. Fennel, D. Vandemark, and M. A. M. Friedrichs (2016), Interannual and seasonal variabilities in air-sea CO_2 fluxes along the U.S. eastern continental shelf and their sensitivity to increasing air temperatures and variable winds, *J. Geophys. Res. Biogeosci.*, *121*, doi:10.1002/2015JG002939.

Received 30 JAN 2015
Accepted 19 DEC 2015
Accepted article online 28 DEC 2015

Interannual and seasonal variabilities in air-sea CO_2 fluxes along the U.S. eastern continental shelf and their sensitivity to increasing air temperatures and variable winds

Bronwyn Cahill[1], John Wilkin[2], Katja Fennel[3], Doug Vandemark[4], and Marjorie A. M. Friedrichs[5]

[1]Informus GmbH, Berlin, Germany, [2]Institute of Marine and Coastal Sciences, Rutgers State University of New Jersey, New Brunswick, New Jersey, USA, [3]Department of Oceanography, Dalhousie University, Halifax, Nova Scotia, Canada, [4]OPAL, EOS, University of New Hampshire, Durham, New Hampshire, USA, [5]Virginia Institute of Marine Science, College of William & Mary, Gloucester Point, Virginia, USA

Abstract Uncertainty in continental shelf air-sea CO_2 fluxes motivated us to investigate the impact of interannual and seasonal variabilities in atmospheric forcing on the capacity of three shelf regions along the U.S. eastern continental shelf to act as a sink or source of atmospheric CO_2. Our study uses a coupled biogeochemical-circulation model to simulate scenarios of "present-day" and "future-perturbed" mesoscale forcing variability. Overall, the U.S. eastern continental shelf acts as a sink for atmospheric CO_2. There is a clear gradient in air-sea CO_2 flux along the shelf region, with estimates ranging from $-0.6\,\mathrm{Mt\,C\,yr^{-1}}$ in the South Atlantic Bight (SAB) to $-1.0\,\mathrm{Mt\,C\,yr^{-1}}$ in the Mid-Atlantic Bight (MAB) and $-2.5\,\mathrm{Mt\,C\,yr^{-1}}$ in the Gulf of Maine (GOM). These fluxes are associated with considerable interannual variability, with the largest interannual signal exhibited in the Gulf of Maine. Seasonal variability in the fluxes is also evident, with autumn and winter being the strongest CO_2 sink periods and summer months exhibiting some outgassing. In our future-perturbed scenario spatial differences tend to cancel each other out when the fluxes are integrated over the MAB and GOM, resulting in only minor differences between future-perturbed and present-day air-sea CO_2 fluxes. This is not the case in the SAB where the position of the along-shelf gradient shifts northward and the SAB becomes a source of CO_2 to the atmosphere ($0.7\,\mathrm{Mt\,C\,yr^{-1}}$) primarily in response to surface warming. Our results highlight the importance of temperature in regulating air-sea CO_2 flux variability.

1. Introduction

The flux of CO_2 between the atmosphere and the ocean is a critical process in the global carbon cycle, yet significant uncertainty in estimates of this flux stem from the portion associated with uptake and release of CO_2 on continental shelves. Globally, it is estimated that approximately 26% (or $2.3 \pm 0.4\,\mathrm{Pg\,C\,yr^{-1}}$) of CO_2 presently emitted as a result of anthropogenic activities is absorbed by the world ocean [*Le Quéré et al.*, 2009, 2010]. In the open ocean, *Takahashi et al.* [2009] estimate a contemporary sink of atmospheric CO_2 of $-1.6 \pm 0.9\,\mathrm{Pg\,C\,yr^{-1}}$. In the coastal ocean, *Laruelle et al.* [2014] have recently evaluated the flux of CO_2 as a sink of atmospheric CO_2 of $-0.19 \pm 0.05\,\mathrm{Pg\,C\,yr^{-1}}$. While this corresponds to 8% (or 14%) of the open ocean sink, its significance is clouded by major uncertainties associated with the estimates. Regional quantification and global extrapolation of coastal fluxes are uncertain due to spatial and temporal variabilities and undersampling [*Fennel*, 2010].

High productivity on shelf systems is driven by the interplay between temperature, light, and nutrient inputs from land, remineralization in shelf sediments due to tight benthic-pelagic coupling that returns nutrients to the euphotic zone on time scales on the order of a year and most importantly by upwelling and onwelling of nutrients from the open ocean. However, not all continental shelf systems respond in the same manner to these drivers and there are wide regional differences in continental shelves' potential to be a source or sink for atmospheric CO_2 [*Cai et al.*, 2006; *Borges*, 2011; *Borges et al.*, 2005]. This makes it important to view regions as distinct provinces.

Evaluating and understanding air-sea CO_2 fluxes on the scale of continental shelves is difficult; we adopt an approach that combines model experiments with the analysis of in situ data and considers ocean circulation, primary production, and geochemistry. A key factor influencing variability of air-sea CO_2 fluxes in shelf regions is atmospheric forcing. In this study, we investigate the impact of interannual and seasonal variabilities in atmospheric forcing on the capacity of different shelf subregions to act as a sink or source of atmospheric CO_2. We

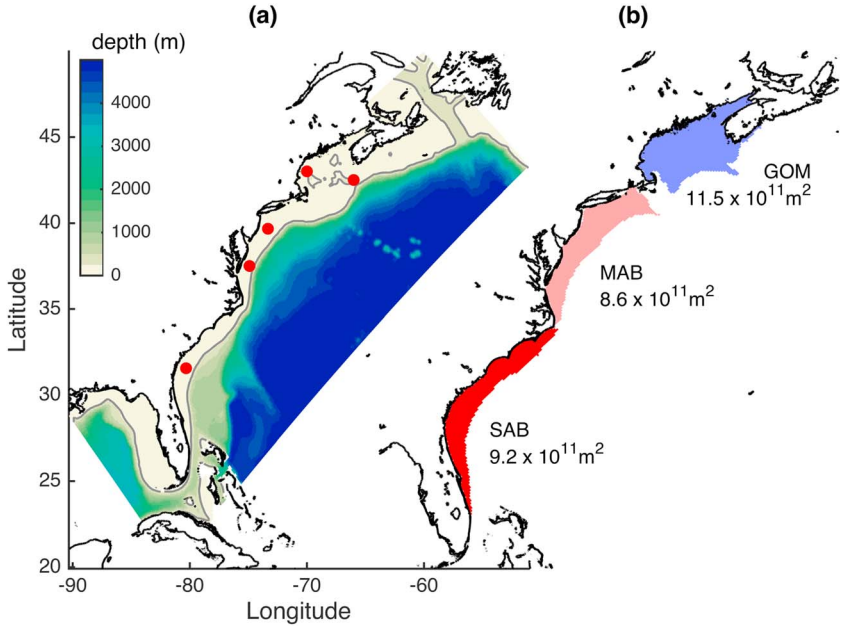

Figure 1. (a) Study location, model domain, and location of observations (red circles) used in the analyses (black contour denotes the location of 200 m isobath) and (b) boundaries and surface area of the analysis regions, Gulf of Maine (GOM), Mid-Atlantic Bight (MAB), and South Atlantic Bight (SAB).

assess the "present-day" response of different shelf subregions to contemporary atmospheric forcing and evaluate the sensitivity of regional air-sea CO_2 fluxes to a "future-perturbed" scenario where the present-day atmospheric forcing is perturbed with atmospheric anomalies derived from modern and future scenarios of a regional climate model (RegCM3). We focus only on changes in atmospheric forcing and do not take into account changes in river inputs, projected future ocean biogeochemical state, or higher atmospheric pCO_2 (pCO_2^{AIR}). We assume, to first order, that the rate of change in pCO_2^{SEA} in the coastal ocean is tracking the rate of pCO_2^{AIR} increase, so that the air-sea gradient of CO_2 does not change over time, at least for surface waters, between our present-day and future-perturbed scenarios. We provide further details in section 3.2 explaining the reasons justifying this assumption.

The rest of the paper is organized as follows: in section 2, we present the overall study region; the Northeast North American shelf; and the different characteristics of three subregions under investigation: Gulf of Maine, Mid-Atlantic Bight, and South Atlantic Bight. In section 3, we present the biogeochemical model, the configuration of our model experiments, and the approach to our sensitivity analysis. In the first part of section 4, we present the model results and an assessment of present-day seasonal and interannual air-sea CO_2 fluxes for the three subregions, including an evaluation of the modeled fluxes in comparison to observations. In the second part of section 4, we present the results of a sensitivity analysis and the subregional responses to future-perturbed variations in atmospheric forcing. A discussion and conclusions are presented in section 5.

2. Study Location

The area of interest is the Northeast North American (NENA) continental shelf region along the eastern seaboard of the United States (Figure 1a). Three subregions have been selected for detailed analysis (Figure 1b). These are the Gulf of Maine (GOM), the Mid-Atlantic Bight (MAB), and the South Atlantic Bight (SAB). The choice of boundaries circumscribing each of these regions is broadly determined by the differences in their physical and biological regimes and the 200 m bathymetric contour. They are consistent with those used in *Hofmann et al.* [2011] and *Fennel* [2010]. Primary productivity is high in all three regions, but they have distinct characteristics that make them suitable candidates for evaluating the response of air-sea CO_2 fluxes to different regimes.

2.1. Gulf of Maine

The Gulf of Maine (GOM) is a marginal sea at temperate latitudes in the Northwest Atlantic bounded by Cape Cod to the south and Nova Scotia to the east and separated from the open ocean by Georges Bank and

Browns Bank. With the exception of the Boston region, the coastal watershed is sparsely populated and distinctively rural along much of the coastline. There is a seasonal cycle in stratification and significant primary productivity ($>270\,g\,cm^{-2}\,yr^{-1}$) [*O'Reilly and Busch*, 1984; *Balch et al*., 2008]. Seasonal and interannual circulation variabilities are attributed to variations in shelf-sea exchange through the narrow Northeast Channel and fresher coastal source waters from along the Scotian Shelf [*Townsend*, 1991; *Townsend et al*., 2006; *Pringle*, 2006]. Physical ocean circulation characteristics include a large semidiurnal tide, a persistent counterclockwise gyre circulation with several distinct coastal currents [*Pettigrew et al*., 2005], uneven coastline and bathymetry, and large seasonal freshwater inflow [*Salisbury et al*., 2008]. The western Gulf of Maine is seasonally stratified with heat and buoyancy fluxes exceeding tidal and wind-driven mixing forces from roughly March to November each year. The region is also regularly impacted by local and distant river runoff from April to July, with a resulting increase in buoyancy flux and coastal current velocities [*Geyer et al*., 2004; *Salisbury et al*., 2008] and decrease in surface water residence times [*Manning et al*., 2009]. There is significant carbon input to the GOM from rivers, and temperature, tidal, and wind dynamics all conspire to regulate air-sea CO_2 fluxes in the region [*Vandemark et al*., 2011].

2.2. Mid-Atlantic Bight

The Mid-Atlantic Bight (MAB) is a highly productive ($>310\,g\,cm^{-2}\,yr^{-1}$) [*O'Reilly et al*., 1987] broad continental shelf characterized by consistently high-chlorophyll biomass ($>1\,mg\,chlorophyll\,m^{-3}$) which supports a diverse food web that includes abundant fin and shellfish populations [*Yoder et al*., 2001]. It extends from Cape Cod, Massachusetts, southward to Cape Hatteras, North Carolina, and extends offshore for several hundreds of kilometers. It drains much of the northeast and Mid-Atlantic U.S. including three major watersheds that flow into the Chesapeake Bay, Delaware Bay, and Hudson Estuary, all of which ultimately discharge freshwater, nutrients and organic carbon to the MAB. It is a densely populated, highly urbanized region. Chesapeake Bay is the largest and most productive estuary in the U.S. Its drainage basin extends from New York to Virginia ($171{,}990\,km^2$; ~60% forested), and it discharges more freshwater (mean annual discharge of $2280\,m^3\,s^{-1}$ [*Schubel and Pritchard*, 1986]) than any other river/estuary system along the U.S. Atlantic coast, contributing about half the freshwater that flows into the MAB. The discharge from the Hudson-Raritan estuary system adjacent to New York City accounts for ~20% of the freshwater received by the MAB [*Taylor et al*., 2003], while the urbanized Delaware Estuary has a mean annual freshwater discharge of $550\,m^3\,s^{-1}$ [*Lebo and Sharp*, 1993], contributing ~15–20% of the freshwater discharge entering the MAB.

The waters of the MAB exhibit pronounced seasonal and interannual variabilities in temperature and salinity [*Mountain*, 2003]. In late spring and early summer, a strong thermocline (water temperatures can span from 30 to 8°C in <5 m) develops at about the 20 m isobath across the entire shelf, isolating a continuous midshelf "cold pool" (formed in winter months) that extends from Nantucket to Cape Hatteras [*Houghton et al*., 1982; *Biscaye et al*., 1994]. The cold pool persists throughout the summer until fall when the water column overturns and mixes [*Houghton et al*., 1982]. Thermal stratification redevelops in spring as the frequency of winter storms decrease and surface heat flux increases [*Lentz et al*., 2003].

2.3. South Atlantic Bight

The South Atlantic Bight (SAB) extends along the southeastern United States coast from West Palm Beach, Florida, to Cape Hatteras, North Carolina. It is characterized by a narrow, shallow shelf with the Gulf Stream flowing northward in close proximity to the shelf break. A series of barrier islands delimit the shoreline with extensive salt marshes. The inner shelf (<20 m) is typically influenced by discharge from rivers and marshes. There are 11 rivers that input approximately $66\,km^3$ freshwater annually into the South Atlantic Bight [*Menzel*, 1993]. River discharge usually peaks between February and April and is at a minimum between September and November. The release of groundwater from salt marshes also contributes to the freshwater input into the region, although this flux is poorly quantified. The total input of organic carbon from marshes and rivers in the South Atlantic Bight is the highest along the U.S. East Coast [*Hopkinson*, 1985; *Wang and Cai*, 2004]. The middle (20–40 m) and outer shelves (40–60 m) are influenced less by river discharge and more by nutrient-rich water intrusions occurring within a semipermanent gyre that exists downstream of the bathymetric feature called the "Charleston Bump" off Long Bay, South Carolina. This brings nutrient-rich water from off the shelf edge and results in enhanced biological production [*Bane and Dewar*, 1988]. Annual primary production estimates are given as $320\,g\,cm^{-2}\,yr^{-1}$ [*Menzel*, 1993].

The annual temperature cycle in the SAB exhibits important seasonal characteristics. Sea surface temperature is relatively uniform over the whole shelf in summer, between 28°C and 31°C in July; however, large cross-shelf gradients in sea surface temperature persist in the winter, ranging from 10°C on the inner shelf to 25°C on the outer shelf [*Jiang et al*., 2008].

3. Model

3.1. NENA Model

The NENA model was developed to investigate the transport and cycling of carbon and nitrogen to and within the U.S. East Coast coastal ocean margin and the impact of climate variability, climate change, and land cover/land use change on these fluxes [*Fennel et al*., 2006; *Hofmann et al*., 2008, 2011]. NENA is based on the Regional Ocean Modeling System (ROMS) and a coupled biogeochemical module. ROMS is widely used for shelf circulation and coupled physical-biological applications [e.g., *Dinniman et al*., 2003; *Lutjeharms et al*., 2003; *Marchesiello et al*., 2003; *Peliz et al*., 2003; *Fennel et al*., 2006, 2008; *Wilkin*, 2006]. The ROMS computational kernel [*Shchepetkin and McWilliams*, 1998, 2003, 2005] produces accurate, conservative evolution of tracer fields, which is a particularly attractive feature for biogeochemical modeling because it facilitates accurate interaction among tracers and accounting of total nutrient and carbon budgets.

The NENA model domain (Figure 1a) encompasses the entire U.S. East Coast continental shelf, which presents a number of challenges in terms of model complexity, boundaries, and resolution. There are 31 rivers represented along the land-ocean boundary, complex open boundaries that include subtropical and subpolar regions of the Atlantic Ocean, and a significant shelf area where sediment-water interactions play an important role [e.g., *Fennel et al*., 2006]. The model configuration used here has a 10 km horizontal resolution and 30 terrain-following vertical levels stretched to give increased resolution in surface and bottom boundary layers. This is sufficient to capture the dominant dynamics governing shelf-wide circulation. Open boundary temperature, salinity, and subtidal frequency velocity are taken from 5 day averages of the HYbrid Coordinate Ocean Model (HYCOM) data assimilation product developed as part of the Global Ocean Data Assimilation Experiment North Atlantic Basin "best estimate" analysis for 2003 to the present [*Chassignet et al*., 2007]. Tides are introduced at the boundary using harmonic data from the Oregon State University TOPEX/Jason altimeter data inversion [*Egbert and Erofeeva*, 2002] and a surface gravity wave radiation scheme [*Flather*, 1976]. Air-sea heat and momentum fluxes are computed using bulk formulae [*Fairall et al*., 2003] applied to model sea surface conditions and air temperature, pressure, humidity, radiation, precipitation, and winds from 3 h interval National Center for Environmental Prediction North American Regional Reanalysis (NCEP-NARR) [*Mesinger et al*., 2006]. Vertical turbulent mixing closure uses the parameterization of *Mellor and Yamada* [1982] implemented via the *k-kl* option of *Warner et al*. [2005].

The biogeochemical module of the NENA model incorporates carbon and nitrogen dynamics after *Fennel et al*. [2006, 2008] and *Fennel and Wilkin* [2009]. The model currency is nitrogen with an assumed fixed C:N ratio for plankton but independent C and N state variables for detritus. Particulate flux to the seabed is partly recycled and partly lost to N_2 gas via an explicit sediment denitrification parameterization. The Ocean Carbon Cycle Model Intercomparison Project standard is used for the carbonate system and the *Wanninkhof* [1992] formulation for gas exchange. Atmospheric pCO_2^{AIR} is fixed at 377.4 ppm. Boundary estimates for nitrate, dissolved inorganic carbon (DIC), total alkalinity (TA), and oxygen were derived using temperature and salinity data from the World Ocean Atlas [*Conkright et al*., 2002] and property-property relationships, which account for regional differences in the subpolar and subtropical regions based on *Fennel et al*. [2008], *Lee et al*. [2000], and *Millero et al*. [1998]. Inputs from 31 rivers are prescribed as a point source climatology derived from U.S. Geological Survey freshwater gauge data after *Howarth et al*. [2000], essentially representing net freshwater and biogeochemical (total nitrogen in the nitrate pool) transport into the coastal ocean. There is no interannual variability in our river inputs.

3.2. Model Experiments

Two model scenarios were developed and run for a 4 year period corresponding to 2004 to 2007 (Table 1). The first scenario, referred to as present day, represents contemporary mesoscale variability in forcing as captured by NARR-NCEP 3 hourly meteorology fields from 2004 to 2007. The year 2004 corresponds to a positive North Atlantic Oscillation (NAO) index, while 2005 to 2007 corresponds with a negative NAO index. The difference between the positive and negative NAO periods is evident in the wind data, where the Gulf of Maine

Table 1. Configuration of "Present-Day" and "Future-Perturbed" Scenarios

	Present Day	Future Perturbed
Atmospheric forcing	NCEP-NARR 3 h fields •T_{AIR} •P_{AIR} •Q_{AIR} •RAIN •SWRAD •LWRAD •U_{WIND} •V_{WIND}	Atmospheric anomalies were added to present-day NCEP-NARR fields. Anomalies were derived from two 10 year simulations of RegCM3 model [*Chen et al.*, 2003] representing present and end of century (doubled) CO_2 levels, forced by 100 year transient run of NCAR climate system model
pCO_2^{AIR}	377.4 ppmv	
Time period	4 years corresponding to 2004 to 2007	

and Mid-Atlantic Bight experience pronounced northeasterly winds in 2004, as compared to pronounced easterly winds in these regions in subsequent years (not shown).

The second scenario, referred to as future perturbed, adjusts the present-day forcing by adding atmospheric forcing anomalies derived from modern and future scenarios of a regional climate model, RegCM3, indicative of a doubling of atmospheric CO_2. River inputs remain the same as in the present-day scenario. We intentionally do not have any future-perturbed signal in the river inputs because we want to isolate the impact of atmospheric variability on air-sea CO_2 fluxes.

The concentration pCO_2^{AIR} was kept at 377.4 ppm, as in the present-day scenario for several important reasons. We do not take into account the projected biogeochemical ocean state because of the absence of robust, regional future projections of ocean state required to initialize a future air-sea biogeochemical equilibrium. We note that Earth system models (ESMs) which have run coupled biophysical projections of future ocean state (i.e., various Intergovernmental Panel on Climate Change (IPCC) scenarios) are typically global simulations where the biogeochemical equilibrium is maintained throughout the duration of the simulation (from present to future). In other words, the biogeochemical ocean state evolves in concert with increasing atmospheric CO_2 concentrations and is not abruptly imposed in a regional context, at some point in the future, as would be the case if we were to double the concentration of pCO_2^{AIR} in our future-perturbed scenario. Moreover, global ESM simulations do not capture the open ocean mesoscale dynamics or coastal boundary current inflows from the north (Labrador) and south (Gulf of Mexico) that we need to use in our regional model context. A recent comparison of selected physical variables for the NW Atlantic from historical and future simulations (IPCC RCP4.5 and RCP8.5) from six ESMs indicates that all six models have a poor representation of the detailed structure of important ocean and ice features. Furthermore, it is doubtful whether any of the models have an adequate representation of regional ocean dynamics to reliably simulate ocean climate variability and change. The magnitudes of the intermodel differences in the projected changes are comparable to those of the ensemble mean changes, such that it is not possible to make any robust quantitative projections at a regional scale, yet it is unclear whether any of the models examined are worse than the others to the point that they should be rejected from an ensemble approach to climate change projections [*Loder and van der Baaren*, 2013]. Instead, we assume to first order that the rate of change in pCO_2^{SEA} in the coastal ocean is tracking the rate of pCO_2^{AIR} increase, so that the air-sea gradient of CO_2 does not change over time, at least for surface waters, which is consistent with the space and time scales of our study.

As an added check, we looked into the potential impact on air-sea flux from a Revelle factor change due to an order of +100 ppmv change in atmospheric CO_2 in this region. We find a small increase in the surface Revelle factor in the SAB (approximately 2%) and even less in the MAB and GOM regions (±0.5%). While this could impact solubility by a small amount from one scenario to another (e.g., due to changes in temperature), the net impact on our study conclusions appears to be quite small.

The main features of the atmospheric anomalies imposed in the future-perturbed scenario are found in the air temperature and wind anomalies. There is an overall increase in air temperature over the entire model domain ranging from 1°C offshore to as much as 3°C along coastal regions. This will have important consequences for the modeled surface temperature and pCO_2^{SEA}. There is also a decrease in the northeasterly wind component in the Gulf of Maine and northern Mid-Atlantic Bight, an increase in the easterly wind component in the southern Mid-Atlantic Bight, and an increase in the southeasterly wind component in the South Atlantic Bight (Figure 2).

3.3. Sensitivity Analysis

The modeled local rate of change of DIC accounts for biogeochemical sources and sinks, advection and diffusion by ocean circulation, and the exchange of CO_2 gas across the air-sea interface. Schematically, this modeled rate may be described as

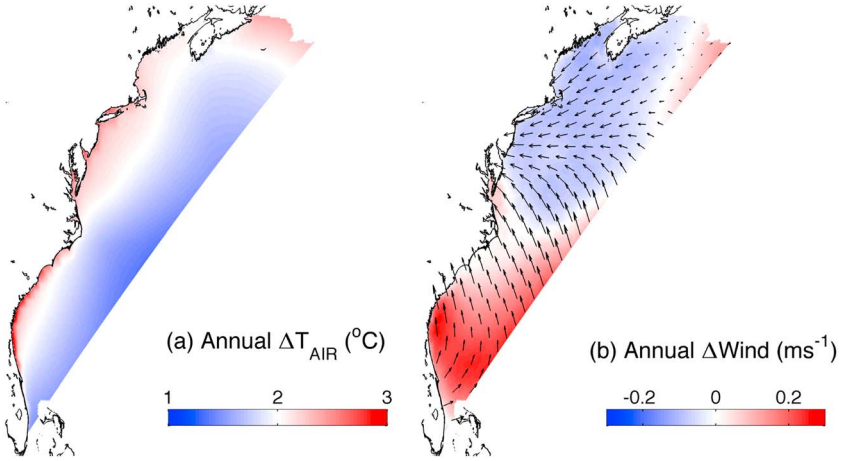

Figure 2. RegCM3-derived (a) annual air temperature and (b) wind speed atmospheric anomalies.

$$\begin{aligned}\partial \mathrm{DIC}/\partial t = &\ -\text{nutrient-based uptake by phytoplankton}\\ &+\text{excretion (due to basal metabolism and grazing dependence)}\\ &+\text{solubilization of detritus small and large}\\ &-\text{advection} + \text{diffusion} + \text{air-sea flux of } CO_2\end{aligned}$$

Details on the parameterization of the biogeochemical processes are given by *Fennel et al*. [2006, 2008] and *Druon et al*. [2010].

The air-sea flux of CO_2 is parameterized by

$$F = \frac{\mathrm{kw}^2}{\mathrm{Sc}^{1/2}\Delta z}\mathrm{CO}_2^{\mathrm{SOL}}\left(p\mathrm{CO}_2^{\mathrm{AIR}} - p\mathrm{CO}_2^{\mathrm{SEA}}\right) \quad (1)$$

which is a function of wind speed, w; the Schmidt number (Sc) for CO_2 which depends on temperature, T; the solubility of CO_2 (a function of T and S); and the air-sea CO_2 partial pressure difference (a function of T, S, TA, and DIC). Δz represents the thickness of the top model grid box. In order to explore the sensitivity of air-sea CO_2 fluxes to variability in atmospheric forcing, we examine the contributions of these four terms to the change in air-sea CO_2 flux between our "present-day" and "future-perturbed" scenarios. We note that our choice of the *Wanninkhof* [1992] gas transfer parameterization, k, predates more recent developments and improvements in this field [*Wanninkhof*, 2014]. The uncertainty associated with the choice of gas transfer velocity formulation is estimated to be around 10% for wind speeds between 3 and 12 ms^{-1} [*Ho et al*., 2011; *Sweeney et al*., 2007; *Nightingale et al*., 2000a, 2000b] and as much as 20% for wind speeds >12 ms^{-1} [*Wanninkhof*, 2014].

Following the methodology of *Previdi et al*. [2009], we express the difference δF in the CO_2 flux using first- and second-order Taylor series approximations. We estimate the linear sensitivity of F to changes in forcing from first-order partial derivatives (equation (2)) and the nonlinear effects contributing to δF by computing second-order partial derivatives (equation (3)).

The first-order partial derivatives are approximated using a method of single field substitution:

$$\frac{\partial F}{\partial X_i}\delta X_i \approx F\left(\underline{X}^{\mathrm{FUTURE}} + \underline{e}_i \Delta \underline{X}\right) - F\left(\underline{X}^{\mathrm{FUTURE}}\right) \quad (2)$$

where the first term on the right-hand side is calculated using the time series of variable X_i from the present-day scenario in the term $\Delta\underline{X}$ and the time series of all other variables from the future-perturbed scenario in the term $\underline{X}^{\mathrm{FUTURE}}$. In the second term on the right-hand side of equation (2), all variables in the term $\underline{X}^{\mathrm{FUTURE}}$ are from the future-perturbed model scenario. This approach was introduced in meteorological studies of cloud radiative feedback by *Wetherald and Manabe* [1988] and *Colman et al*. [1997]. It provides an estimate of the linear sensitivity of F to various changes in the system; here the change in F is due to a change in wind speed, Schmidt number, CO_2 solubility, or $p\mathrm{CO}_2^{\mathrm{SEA}}$ alone.

Nonlinear effects contributing to δF are estimated by computing second-order partial derivatives. These higher-order derivatives are approximated as

$$\begin{aligned}\frac{\partial^2 F}{\partial X_i \partial X_j}\delta X_i \delta X_j \approx &\left(F\left(\underline{X}^{\mathrm{FUTURE}}+\left(\underline{e_i}+\underline{e_j}\right)\Delta\underline{X}\right)-F\left(\underline{X}^{\mathrm{FUTURE}}+\underline{e_j}\Delta\underline{X}\right)\right)\\ &-\left(F\left(\underline{X}^{\mathrm{FUTURE}}+\underline{e_i}\Delta\underline{X}\right)-F\left(\underline{X}^{\mathrm{FUTURE}}\right)\right)\\ =&\left(F\left(\underline{X}^{\mathrm{FUTURE}}+\left(\underline{e_i}+\underline{e_j}\right)\Delta\underline{X}\right)-F\left(\underline{X}^{\mathrm{FUTURE}}+\underline{e_j}\Delta\underline{X}\right)\right)-\frac{\partial F}{\partial X_i}\delta X_i\end{aligned} \tag{3}$$

where, again using single field substitution, $F(X^{\mathrm{FUTURE}}+(e_i+e_j)\Delta X)$ was calculated using the time series of X_i and X_j from the present-day scenario, in the term $\Delta\underline{X}$, and the time series of all other variables from the future-perturbed scenario, in the term $\underline{X}^{\mathrm{FUTURE}}$. The values calculated in equation (3) indicate how the sensitivity of F to changes in X_i depends on X_j or, more generally, how this sensitivity depends on the state of the system. This becomes important in the analysis of the pCO_2^{SEA} contribution to the air-sea CO_2 flux and how the effects of the different processes which control pCO_2^{SEA} (e.g., net ecosystem production and air-sea gas exchange) depend on the state of the system.

4. Results

Previous work on the evaluation of the NENA model supports our confidence in the current estimates of ocean state, including the biogeochemical ocean state [*Fennel et al*., 2006; *Hofmann et al*., 2008; *Previdi et al*., 2009]. Here we focus our evaluation on the modeled air-sea CO_2 fluxes and their subsequent response to perturbations in atmospheric forcing. To clarify the direction of our air-sea CO_2 fluxes, a positive flux indicates that the ocean is acting as a source of CO_2 to the atmosphere, while a negative flux indicates that the ocean is acting as a sink of CO_2 from the atmosphere.

4.1. Present Day Air-Sea CO_2 Fluxes

The simulated present-day estimates of air-sea CO_2 fluxes indicate that on an annual time scale, the Gulf of Maine, Mid-Atlantic Bight, and South Atlantic Bight all act as sinks for atmospheric CO_2, with considerable seasonal and spatial variabilities. A clear along-shelf gradient (south to north) in the sign and magnitude of the air-sea CO_2 flux exists throughout the whole NENA shelf region (Figure 3a), consistent with previous descriptions [*Chavez and Takahashi*, 2007]. A cross-shelf gradient also exists in the sign and magnitude of the air-sea CO_2 flux in the South Atlantic and Mid-Atlantic Bights. The inner shelf of the southern part of the South Atlantic Bight acts as a source of CO_2 to the atmosphere, while the middle and outer shelves in the southern SAB act as a mild sink for atmospheric CO_2. This is consistent with the findings of *Jiang et al*. [2008] who report the inner shelf as a source of $+1.2\,\mathrm{mol\,C\,m^{-2}\,yr^{-1}}$ and the middle and outer shelves as sinks of -1.23 and $-1.37\,\mathrm{mol\,C\,m^{-2}\,yr^{-1}}$, respectively. The northern part of the South Atlantic Bight, however, does not reflect this cross-shelf pattern but shows the inner shelf acting as a mild sink of CO_2 from the atmosphere and the middle and outer shelves as more or less neutral. Most of the river runoff in the SAB is distributed between 31°N and 33°N, with the southern portion of the SAB receiving the least water from rivers [*Jiang et al*., 2008]. Most likely, our result indicates that we are not resolving the input of organic carbon from marshes and rivers sufficiently in the model in the northern part of the South Atlantic Bight.

The cross-shelf gradient in the Mid-Atlantic Bight is much more consistent with observations. Coastal areas of the Mid-Atlantic Bight act as a source of CO_2 for the atmosphere, while the Mid-Atlantic Bight shelf and slope waters and the Gulf of Maine act as stronger sinks of atmospheric CO_2. A larger interannual variability in air-sea CO_2 fluxes is evident between 2004 and the subsequent model years (2005–2007), especially in the Gulf of Maine (Figure 3c), possibly in response to NAO-driven variability in atmospheric forcing between 2004 (positive NAO index) and 2005 to 2007 (negative NAO index).

The annual mean estimates of air-sea CO_2 fluxes show a seasonal cycle within each of the subregions supported by the seasonal cycles of surface temperature, pCO_2^{SEA}, and primary production (Figures 4–6). Autumn and winter are the strongest CO_2 sink periods, corresponding with lower pCO_2^{SEA} values driven by lower surface

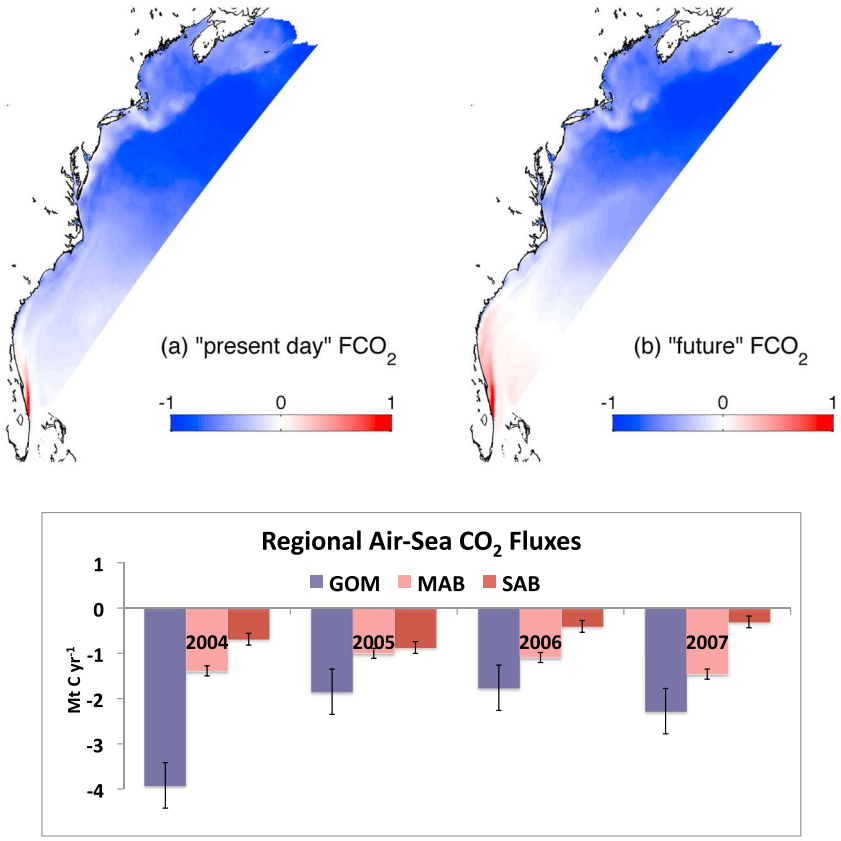

Figure 3. Four-year mean (a) "present-day" and (b) "future-perturbed" air-sea CO_2 flux, FCO_2 (mol C m^{-2} yr^{-1}). (c) Interannual air-sea CO_2 flux, FCO_2 (Mt C yr^{-1}).

temperatures. Some outgassing occur during the summer months (June to August) when surface warming tends to increase pCO_2^{SEA}, thus decreasing the uptake of atmospheric CO_2.

The present-day estimates of annual air-sea CO_2 fluxes agree well with observed and calculated estimates within the MAB and SAB subregions [*Takahashi et al*., 2009; *Jiang et al*., 2008] (Table 2). This is also supported by good agreement between the modeled and observed mean pCO_2^{SEA} (Figures 5a and 5b and 6a and 6b). Various other estimates of air-sea CO_2 fluxes for the MAB (−0.6 to −1.7 mol C m^{-2} yr^{-1}) (*Signorini et al*., 2013; *Fennel et al*., 2008; *Previdi et al*., 2009; *DeGrandpre et al*., 2002) and SAB (−0.79 mol C m^{-2} yr^{-1}) [*Signorini et al*., 2013] regions are also consistent with our modeled estimates. The model seems to capture both the magnitude of the annual air-sea CO_2 flux and also its seasonal cycle for both the Mid-Atlantic Bight and the South Atlantic Bight. This is not the case for the Gulf of Maine, where the annually integrated model results indicate that the region acts as a sink for CO_2 (−1.8 mol C m^{-2} yr^{-1}). Observations from a coastal station coincident with the model run period (2004 to 2008) indicate that the region acts as a weak source of CO_2 to the atmosphere (0.34 mol C m^{-2} yr^{-1}) [*Vandemark et al*., 2011]. *Signorini et al*. [2013] also find the Gulf of Maine to be a weak source of CO_2 to the atmosphere (0.11 mol C m^{-2} yr^{-1}). While the model captures the observed summer time air-sea CO_2 flux in the Gulf of Maine very well with respect to *Vandemark et al*. [2011], there is a significant divergence in the flux estimates between the model and observations in autumn and winter where the observations show this to be a period of efflux in the region. This is also reflected between the modeled and observed estimates of pCO_2^{SEA} (Figures 4a and 4b). Spatial variations in pCO_2^{SEA} and air-sea CO_2 fluxes will be greater in the 30–45 day spring and fall periods when the mixed layer is in transition [*Vandemark et al*., 2011; *Salisbury et al*., 2009]. Precipitation and freshwater discharge in spring can lead to freshening and depletion of DIC in surface waters. It is our supposition that the model is not capturing important changes in water mass properties at these transition periods because our initialization of DIC and alkalinity in the Gulf of Maine does not include sufficient samples from the Gulf of Maine. The DIC and TA initial conditions were derived

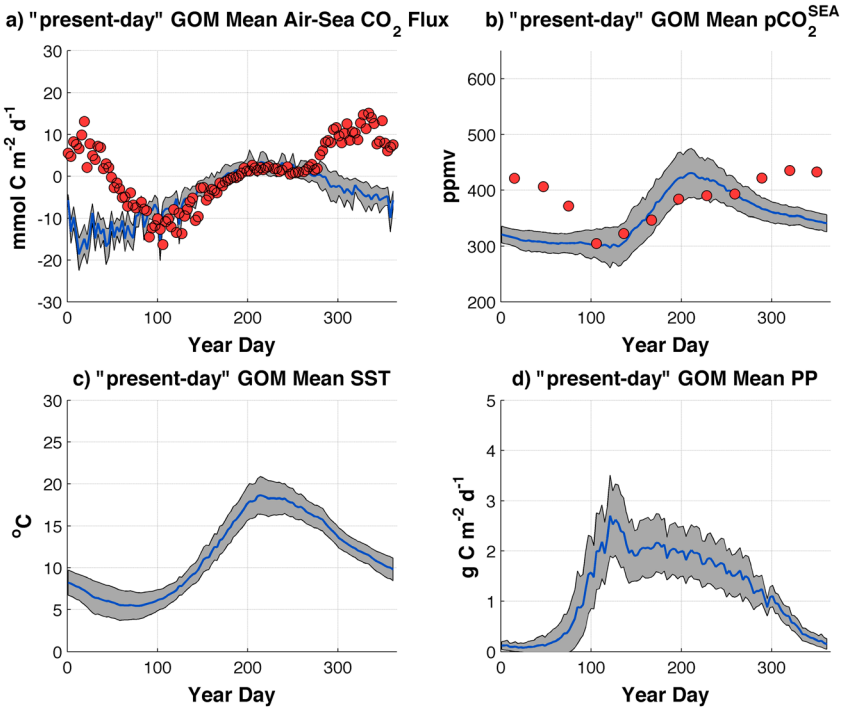

Figure 4. "Present-day" mean (a) air-sea CO_2 fluxes (mmol C m^{-2} d^{-1}), (b) pCO_2^{SEA} (ppmv), (c) SST (°C), and (d) primary production (g C m^{-2} d^{-1}) in the Gulf of Maine (shaded area indicates the standard deviation, and red dots indicate the observations from *Vandemark et al.* [2011]).

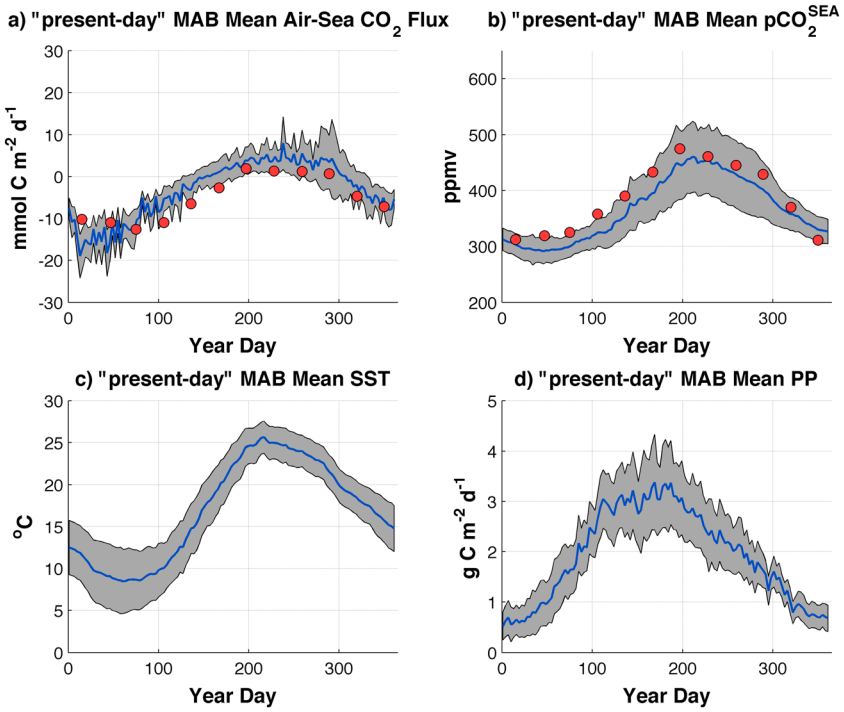

Figure 5. "Present-day" mean (a) air-sea CO_2 fluxes (mmol C m^{-2} d^{-1}), (b) pCO_2^{SEA} (ppmv), (c) SST (°C), and (d) primary production (g C m^{-2} d^{-1}) in the Mid-Atlantic Bight (shaded area indicates the standard deviation, and red dots indicate the observations from *Takahashi et al.* [2009]).

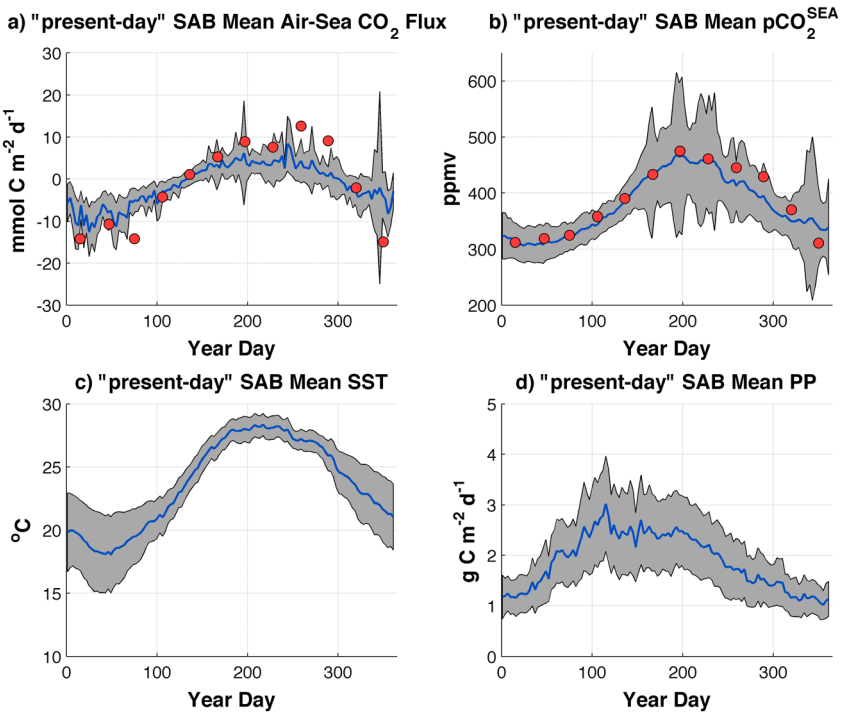

Figure 6. "Present-day" mean (a) air-sea CO_2 fluxes (mmol C m^{-2} d^{-1}), (b) pCO_2^{SEA} (ppmv), (c) SST (°C), and (d) primary production (g C m^{-2} d^{-1}) in the South Atlantic Bight (shaded area indicates the standard deviation, and red dots indicate the observations from *Jiang et al*. [2008]).

using property-property relationships developed by *Lee et al*. [2000] for DIC and by *Millero et al*. [1998] for alkalinity, with temperature and salinity data collected between 1981 and 1998 and between 1980 and 1986, respectively. What we believe we are seeing in our results for the GOM is the sensitivity of this region to these fields and how the Lee and Millero relationships are based on databases that do not have sufficiently high sampling in the GOM region to capture its distinct water mass properties. This has highlighted the need for a regionally specific initialization in the Gulf of Maine with respect to DIC and alkalinity, something that is currently being investigated beyond this study.

4.2. Future-Perturbed Air-Sea CO_2 Fluxes and Sensitivity Analysis

The response of the air-sea CO_2 flux to future-perturbed variations in atmospheric forcing (Figure 3b) is evaluated by examining the magnitude of the difference between the 4 year mean fluxes for each model scenario (Figure 7a). The intention here is to remove the long-term climate variability and focus just on the changes that occur with long-term climate change as represented by the RegCM3-derived atmospheric anomalies. The main differences in the future-perturbed atmospheric forcing fields are found in the air temperature and wind forcing. There is an overall increase in air temperature over the entire model domain ranging from

Table 2. Interannual "Present-Day" Air-Sea CO_2 Fluxes (mol C m^{-2} yr^{-1}) (Positive Flux Indicates That the Ocean Acts as a Source of CO_2 to the Atmosphere, and Negative Flux Indicates That the Ocean Acts as a Sink of CO_2 From the Atmosphere)

		Air-Sea CO_2 Flux (mol C m^{-2} yr^{-1})					
Region	Area (10^{11} m^2)	2004	2005	2006	2007	Mean (STD)	Obs
GOM	11.5	−2.8	−1.3	−1.3	−1.7	−1.8 (0.7)	0.3[a]
MAB	8.6	−1.4	−1.0	−1.1	−1.4	−1.2 (0.2)	−1.8[b]
SAB	9.2	−0.6	−0.8	−0.4	−0.3	−0.5 (0.2)	−0.5[c]

[a] *Vandemark et al*. [2011].
[b] *Takahashi et al*. [2009].
[c] *Jiang et al*. [2008].

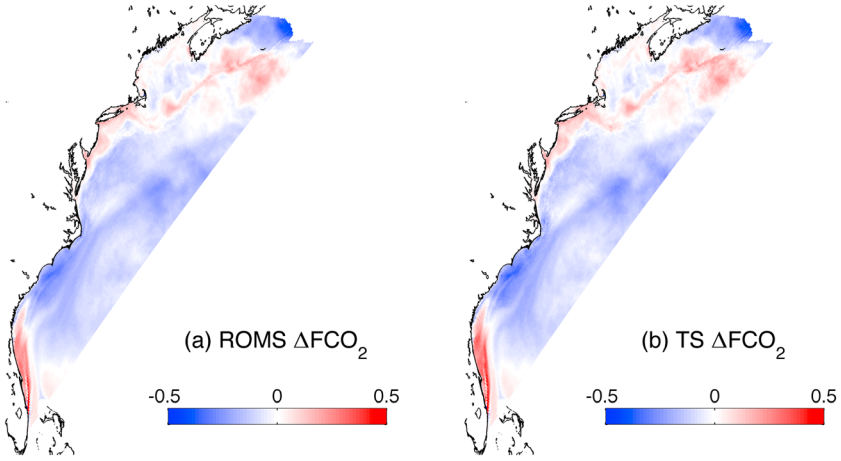

Figure 7. Magnitude of "future-perturbed"-"present-day" (a) ROMS annual air-sea CO_2 flux difference, ΔFCO_2 (mol C m^{-2} yr^{-1}), and (b) first-order Taylor series approximation of annual air-sea CO_2 flux difference, ΔFCO_2 (mol C m^{-2} yr^{-1}).

1°C offshore to as much as 3°C along coastal regions (Figure 2a). There is also a decrease in the northeasterly wind component in the Gulf of Maine and northern Mid-Atlantic Bight, an increase in the easterly wind component in the southern Mid-Atlantic Bight, and an increase in the southeasterly wind component in the South Atlantic Bight (Figure 2b).

Overall, the most notable spatial differences to the air-sea CO_2 flux in response to the future-perturbed scenario occur in the inner Mid-Atlantic Bight and the southern South Atlantic Bight and to a much lesser extent, the southern coastal Gulf of Maine, where the magnitude of the future-perturbed scenario CO_2 flux is larger than that of the present day (Figure 7a). In contrast, in the inner shelf of the northern South Atlantic Bight, the outer Mid-Atlantic Bight shelf, and to a lesser extent, the northern coastal and outer reaches of Gulf of Maine, the magnitude of the future-perturbed scenario CO_2 flux is less than that of the present day. When the flux differences are integrated over each of the subregions, spatial differences tend to cancel each other out in the Gulf of Maine and Mid-Atlantic Bight but not in the South Atlantic Bight where a significant change occurs. The position of the along-shelf gradient in the sign and magnitude of the air-sea CO_2 flux moves further north, and the subregion as a whole shifts from being a mild sink for atmospheric CO_2 (-0.6 Mt C yr^{-1}) to becoming a source of CO_2 (0.7 Mt C yr^{-1}) to the atmosphere in response to the future-perturbed scenario (Figure 3b and Table 3).

The Taylor series decomposition analysis highlights the relative contributions of the air-sea CO_2 flux terms to the change in the flux in CO_2, FCO_2. Figure 7b shows that the first-order Taylor series estimate of the magnitude of the difference between the future-perturbed and present-day scenarios, ΔFCO_2, is a good approximation of the modeled estimates (Figure 7a). The absolute mean difference between Figures 7a and 7b is 6.9 mmol C m^{-2} yr^{-1}.

Examination of the seasonal contribution of the different wind and pCO_2^{SEA} flux terms provides some insight into which processes may be important for each of the regions in driving the seasonality of air-sea CO_2 fluxes (Figure 8). Contributions from the Schmidt number and the solubility of CO_2 to δF are small and cancel each other out (not shown).

Table 3. Four-Year Mean "Present-Day" and "Future-Perturbed" Air-Sea CO_2 Fluxes (mol C m^{-2} yr^{-1} (Mt C yr^{-1}))

		Air-Sea CO_2 Flux (mol C m^{-2} yr^{-1} (Mt C yr^{-1}))		
Region	Area (10^{11} m^2)	Present Day	Future Perturbed	Difference
GOM	11.5	−1.8 (−2.5)	−1.7 (−2.4)	0.1 (0.1)
MAB	8.6	−1.2 (−1.0)	−1.2 (−1.2)	0.0 (−0.2)
SAB	9.2	−0.5 (−0.6)	0.2 (0.7)	0.7 (1.3)

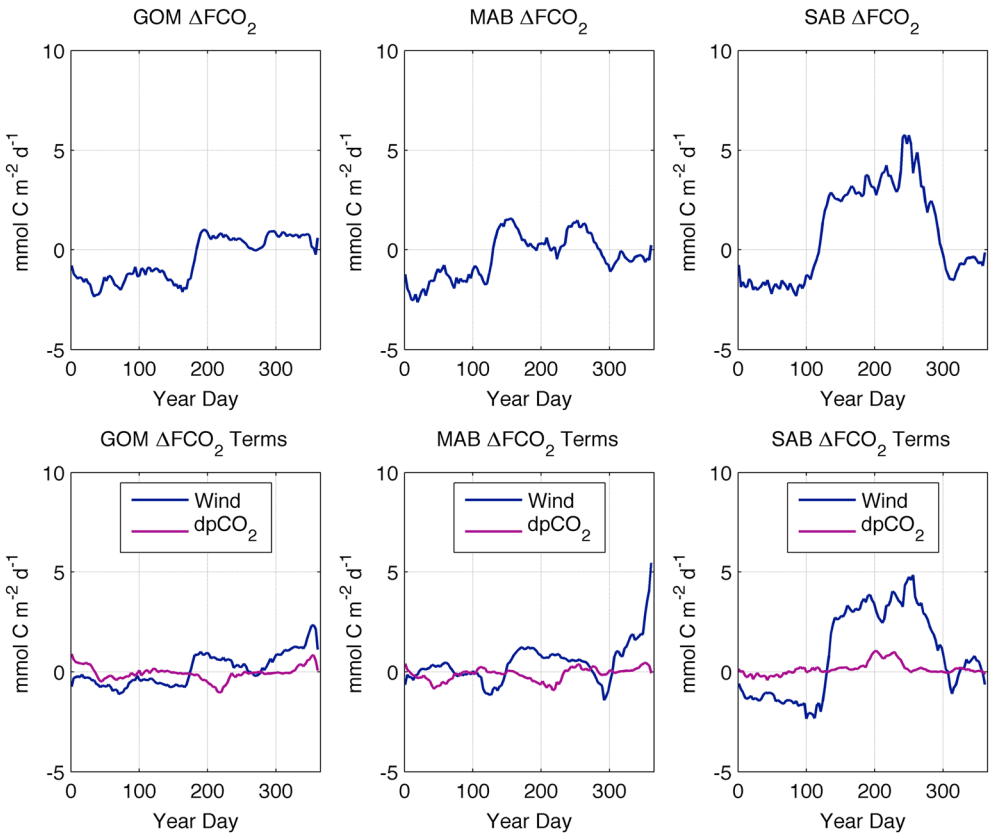

Figure 8. (top row) First-order Taylor series approximations of the magnitude of the mean annually integrated regional flux differences. (bottom row) Magnitude of the mean annually integrated regional flux differences due to changes in pCO_2^{SEA} (red) and flux differences attributable to near-surface (10 m) wind speed changes (blue).

Our analysis of the pCO_2^{SEA} and wind flux terms shows that it is the pCO_2^{SEA} that is dominating the annual FCO_2 response to the future-perturbed scenario, with a lesser contribution from winds (Figure 9). However, winds are playing a stronger seasonal control (Figure 8). This is particularly evident in the South Atlantic Bight in spring and summer when higher sea surface temperatures (SSTs) (acting to increase pCO_2^{SEA}) combined with higher winds contribute to increased outgassing in the region (Figure 3b). That pCO_2^{SEA}

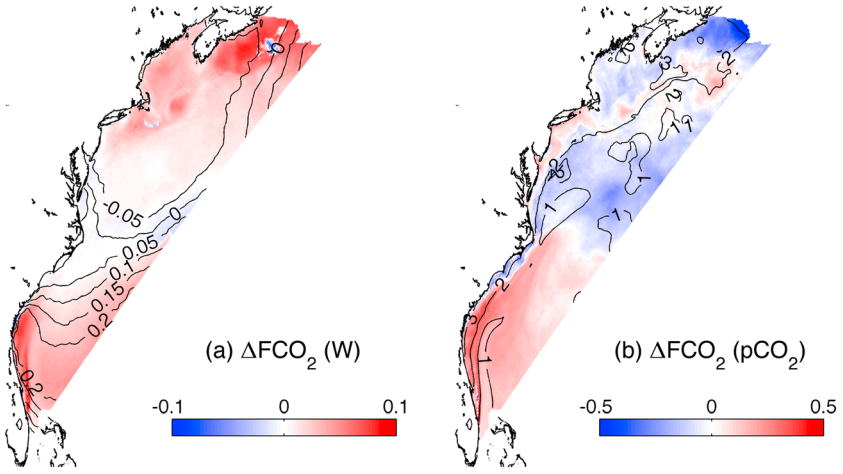

Figure 9. First-order Taylor series approximation of the magnitude of the difference between "future-perturbed" and "present-day" fluxes, ΔFCO_2 (mol C m^{-2} yr^{-1}), (a) magnitude of the annually integrated flux difference attributable to near-surface (10 m) wind speed changes; contours denote the actual annual wind speed difference. (b) Magnitude of the annually integrated flux difference due to changes in pCO_2^{SEA}; contours denote the actual SST differences.

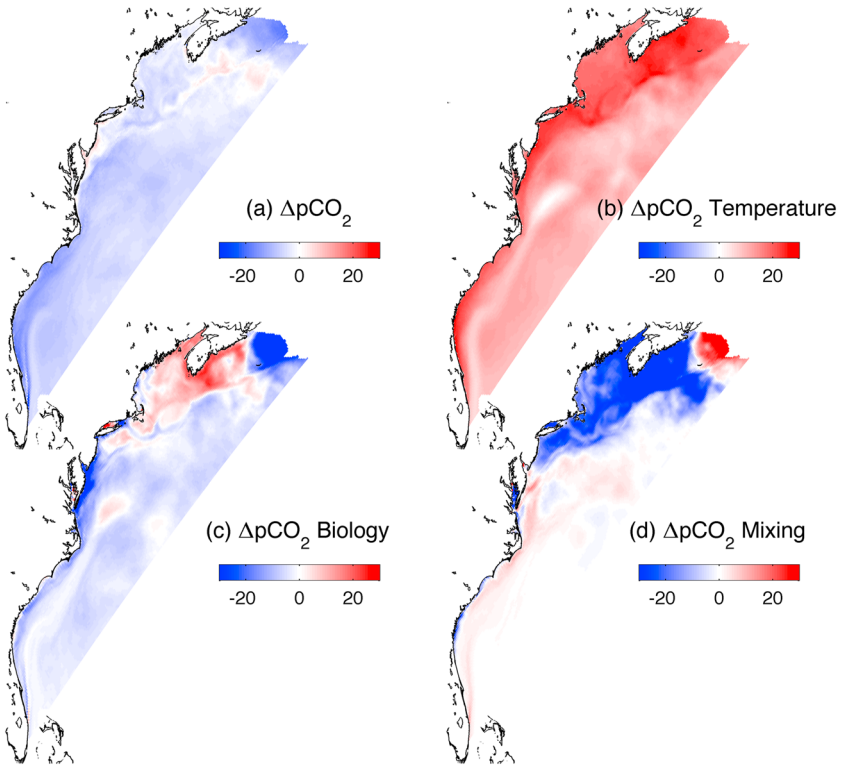

Figure 10. (a) Second-order Taylor series approximation of ΔpCO_2^{SEA} ("future-perturbed"-"present-day"), (b) relative contribution of variations in temperature to ΔpCO_2^{SEA}, (c) relative contribution of variations in biology to ΔpCO_2^{SEA}, and (d) relative contribution of variations in mixing to ΔpCO_2^{SEA}.

dominates the annual response over the entire model domain is not unexpected, given the characteristics of the atmospheric anomalies driving the scenario; i.e., the increase in air temperature will drive an increase in SST which acts to increase pCO_2^{SEA}, thus reducing the uptake of CO_2 by the ocean. Given that our focus here is only on changes in atmospheric forcing and does not take into account a projected future ocean biogeochemical state nor a higher atmospheric pCO_2, the adjustment of pCO_2^{SEA} is a direct response to an increase in SST. However, changes in SST will also have an impact on biological activity and mixing of water masses with different DIC/TA characteristics.

In order to understand the changes to pCO_2^{SEA} which are contributing to δF, we further analyze the Taylor series approximations of the difference in pCO_2^{SEA} due to differences in SST, sea surface salinity, biological activity, and the ratio of mixing of water masses with different DIC/TA characteristics to air-sea CO_2 fluxes (Figure 10). We examine the second-order approximations of pCO_2^{SEA} in this instance because the effects of the different processes that control pCO_2^{SEA} depend on the state of the system.

The negative pCO_2^{SEA} anomalies (Figure 10a) are, for the most part, a clear response to the increase in SST in the future-perturbed perturbation. The contribution of sea surface salinity to pCO_2^{SEA} is not significant (not shown). The relative contribution of biological activity to pCO_2^{SEA} (Figure 10c) is an indication of the effects of anomalous biological activities on DIC and TA pools. It can be interpreted as a sign of net ecosystem production (NEP; net primary production—respiration), in other words, the rate of organic carbon accumulation. Areas of enhanced NEP are associated with a negative biological contribution to the annual mean pCO_2^{SEA} difference, while areas of reduced NEP are associated with a positive biological contribution to the annual mean pCO_2^{SEA} difference [*Previdi et al.*, 2009]. The relative contribution of the ratio of mixing to air-sea CO_2 fluxes on the annual mean pCO_2^{SEA} difference (Figure 10d) effectively balances that from biological activity (Figure 10c). Increased biological production will have the effect of drawing down surface water DIC and decreasing surface pCO_2^{SEA}, thus enhancing atmospheric CO_2 uptake which will counteract the effects of enhanced production. It is the combination of all these three processes (i.e., net effect of biological activity, the ratio of mixing to air-sea CO_2 fluxes, and variability in SST) that is driving the variation in pCO_2^{SEA}. Overall,

we find an approximately 1:1 ratio between temperature and the net effect of biology and mixing, indicating the importance of both processes in controlling the pCO_2^{SEA} variability in our future-perturbed scenario.

5. Discussion and Conclusions

Our assessment of air-sea CO_2 fluxes for three subregions along the U.S. East Coast continental shelf region indicates that annually, all subregions act as a sink for atmospheric CO_2, with some interannual variabilities. The Gulf of Maine exhibits the largest interannual variability, possibly in response to NAO-driven variability in atmospheric forcing.

There is a clear along-shelf gradient in air-sea CO_2 fluxes (south to north) along the whole shelf region with estimates ranging from -0.5 Mt C yr^{-1} in the South Atlantic Bight to -1.0 Mt C yr^{-1} in the Mid-Atlantic Bight and -2.5 Mt C yr^{-1} in the Gulf of Maine. Seasonality in the fluxes is evident, with autumn and winter being the strongest CO_2 sink periods, corresponding with lower pCO_2^{SEA} values driven by lower surface temperatures. During the summer months (June to August), some outgassing occur when surface warming tends to increase pCO_2^{SEA}, thus decreasing the uptake of atmospheric CO_2.

The sensitivity of air-sea CO_2 fluxes to variability in atmospheric forcing shows that an increase in air temperature of up to 3°C in the atmospheric anomalies can have important spatial consequences for the relative contribution of pCO_2^{SEA} to the air-sea CO_2 flux response. To a lesser extent, the increase in northeasterly and southeasterly wind components in the future-perturbed perturbation also had important spatial consequences for the air-sea CO_2 flux response in the Gulf of Maine and South Atlantic Bight, respectively.

Spatial differences tend to cancel each other out when the fluxes are integrated over each of the subregions, except in the South Atlantic Bight where a significant change occurs in response to the future-perturbed perturbation. The position of the along-shelf gradient moves further north, and the subregion experiences a regime shift from being a mild sink for atmospheric CO_2 (-0.6 Mt C yr^{-1}) to becoming a source of CO_2 (0.7 Mt C yr^{-1}) to the atmosphere.

The net effect of variability in biology and the mixing/air-sea CO_2 flux ratio combined with variability in SST are the important processes driving variability in pCO_2^{SEA}. This is consistent with *Signorini et al*. [2013] who showed that changes in DIC and SST are the main factors driving seasonality in pCO_2^{SEA}. *Vandemark et al*. [2011] found that the net effect of biological activity and the ratio of mixing to air-sea CO_2 fluxes was the greater control over variations in pCO_2^{SEA} in late March and into the summer in the Gulf of Maine. Later in the year, temperature and the net effect of biology and mixing were equivalent, indicating that throughout the year, solubility is in competition with other biological and mixing pCO_2^{SEA} controls in the Gulf of Maine. *Jiang et al*. [2008] found a 1:1 ratio between water temperature and all other pCO_2^{SEA} dynamics throughout the year in the South Atlantic Bight and concluded that temperature is the dominant control of pCO_2^{SEA} variability in the South Atlantic Bight. *DeGrandpre et al*. [2002] found a similar temperature-dominated control over pCO_2^{SEA} variability in the Mid-Atlantic Bight. We found that temperature was the dominant control of future-perturbed pCO_2^{SEA} variability for all subregions.

It is likely that our NENA model scenarios are not capturing the complex springtime and late autumn dynamics that regulate pCO_2^{SEA} in the Gulf of Maine. Thus, they are not resolving the competition between solubility and biology/mixing controls in the pCO_2^{SEA} variability in this region. We suppose that the model is not capturing important changes in water mass properties during springtime and winter transition periods because our initialization of DIC and alkalinity in the Gulf of Maine does not include sufficient samples from the Gulf of Maine, highlighting the need for a regionally specific initialization in the Gulf of Maine with respect to DIC and alkalinity. More generally, changes to the water mass properties over the last 40 years, especially a warming and freshening trend in this subregion as a result of climate change, have been reported as virtually certain by the latest IPCC assessment [*Rhein et al*., 2013], suggesting the need to revisit the fitness for purpose of the *Lee et al*. [2000] and *Millero et al*. [1998] regional relationships.

It is worth remembering that our study focuses only on the sensitivity of shelf air-sea CO_2 fluxes to perturbations in atmospheric forcing; however, understanding what drives the response of air-sea CO_2 fluxes in shelf waters, in particular in the context of climate change, is in reality more complicated than this. Our model does not resolve the detailed structure of inland and marsh waters nor does it resolve the complex biogeochemical

transformations that take place in rivers and estuaries prior to reaching the coastal ocean. Nevertheless, we recognize that the impact of changes to riverine inputs is an extremely important and complex problem in itself and the subject of several recent studies. Tao et al. (personal communication) show that river discharge in the region is projected to increase by 40–53% (16–30%) for the IPCC A2 (B1) scenarios by the end of this century. *Herrmann et al*. [2015] show that 60% of the organic carbon entering the U.S. East Coast estuaries actually makes it out to the shelf, while *Laruelle et al*. [2015] highlight how spatial variability in the efficiency of carbon removal through the estuarine filter contributes to the magnitude of the spatial gradient of CO_2 sinks along continental shelf waters of the U.S. East Coast. Their study also reveals that ice and snow cover are important controlling factors of the seasonal dynamics of CO_2 outgassing in rivers and account for significant spatial differences between the Gulf of Maine and Mid-Atlantic Bight regions.

Feng et al. [2015] show that only a fraction of the inorganic nitrogen that enters rivers actually makes it to the shelf and that this fraction has changed a lot over time due to climate change and land use change. Moreover, many of the riverine changes are due to land use changes and it is very difficult to separate the effects of climate change and land use change. *Tian et al*. [2015] have looked at historical changes (1901 to 2008) in riverine carbon inputs specifically for the GOM, MAB, and SAB regions and find significant changes in the DIC flux. In the GOM, they find an increasing DIC trend, while in the MAB and SAB, they find a decreasing DIC trend. No significant change was found in the organic carbon riverine inputs in all regions. Clearly, the impact of climate change on riverine inputs, especially changes to the freshwater input and transport of carbon into the coastal ocean, adds an important layer of complexity to understanding the air-sea flux of CO_2 on the U.S. East Coast continental shelf.

On decadal time scales, studies of the global coupled carbon-climate system suggest that the ocean may become less efficient sink for anthropogenic CO_2 due to positive feedback in the coupled carbon-climate system [*Gruber et al*., 2004]. The amount of DIC in seawater for a given atmospheric partial pressure and ocean total alkalinity is highly temperature dependent. *Gruber et al*. [2004] estimate that a surface ocean warming of 2°C and a 0.5°C warming over the upper 300 m in the next 20 years could lead to an equilibrium loss of about 15 Pg C. Moreover, increases in stratification as a result of increases in upper ocean temperature equivalent to 1.5°C can lead to a reduction in the cumulative uptake of CO_2 by the ocean over 20 years on the order of 10%.

Our study provides a view on how the local response of air-sea CO_2 fluxes to a surface ocean warming of between 2°C and 3°C can differ significantly between subregions. It underlines the role of temperature in regulating pCO_2^{SEA} variability and the complex feedback between solubility and biology/mixing controls. Whereas the South Atlantic Bight shows a shift from being a sink of CO_2 to being a source of CO_2 in its annual air-sea CO_2 flux as a result of surface warming, the Gulf of Maine and Mid-Atlantic Bight show no difference in their annual air-sea CO_2 fluxes. In the South Atlantic Bight where the present-day scenario estimates it as being weak sink of CO_2, variability in winds plays a stronger seasonal control over pCO_2^{SEA} in spring and summer when higher SSTs (acting to increase pCO_2^{SEA}) combined with higher winds are most likely contributing to net annual outgassing in the future-perturbed scenario. While the time frame of our study is too short to qualify as a climate study, it does provide a preliminary indication of the scale of changes to air-sea CO_2 fluxes that may occur as a result of global warming along the U.S. East Coast continental shelf subregions.

Acknowledgments

We would like to thank Dave Pollard for supplying the RegCM3 model output which we used to perturb our future-perturbed scenario and Mike Previdi for providing essential guidance and MATLAB scripts with respect to the Taylor Series decomposition analyses. B.C. would also like to thank Charlie Stock for some very helpful discussions of an early draft of the paper. We gratefully acknowledge the sponsors of the project, the NASA Ocean Biology and Biogeochemistry Program, with funding from both the Interdisciplinary Science and Carbon Cycle Science Program. Finally, we would like to thank two anonymous reviewers whose constructive comments helped to significantly improve our manuscript. Output of the ROMS scenarios used in our analysis is available with unrestricted access from a Rutgers University via Thematic Real-Time Environmental Distributed Data Services (THREDDS) at http://tds.marine.rutgers.edu/thredds/roms/catalog.html. Contact John Wilkin (wilkin@marine.rutgers.edu) for the guidance on which THREDDS entries correspond to the scenarios presented here.

References

Balch, W. M., D. T. Drapeau, B. C. Bowler, E. S. Booth, J. L. Goes, L. A. Windecker, A. Ashe, and J. M. Frye (2008), Space-time variability of carbon standing stocks and fixation rates in the Gulf of Marine, along the GNATS transect between Portland, ME, USA and Yarmouth, Nova Scotia, Canada, *J. Plankton Res.*, *30*(2), 119–139.

Bane, J. M., and J. K. Dewar (1988), Gulf stream bimodality and variability downstream of the Charleston Bump, *J. Geophys. Res.*, *93*, 6695–6710, doi:10.1029/JC093iC06p06695.

Biscaye, P. E., C. N. Flagg, and P. G. Falkowski (1994), The Shelf Edge Exchange Processes experiment, SEEP-II: An introduction to hypotheses, results and conclusions, *Deep Sea Res., Part II*, *41*, 231–252, doi:10.1016/0967-0645(94)90022-1.

Borges, A. V. (2011), Present day carbon dioxide fluxes in the coastal ocean and possible feedbacks under global change, in *Ocean and the Atmospheric Carbon Content*, edited by P. Duarte and J. M. Santana-Casiano, pp. 47–77, Springer, Netherlands.

Borges, A. V., B. Delille, and M. Frankignoulle (2005), Budgeting sinks and sources of CO_2 in the coastal ocean: Diversity of ecosystems counts, *Geophys. Res. Lett.*, *32*, L14601, doi:10.1029/2005GL023053.

Cai, W.-J., M. Dai, and Y. Wang (2006), Air-sea exchange of carbon dioxide in ocean margins: A province based synthesis, *Geophys. Res. Lett.*, *33*, L12603, doi:10.1029/2006GL026219.

Chassignet, E. P., H. E. Hurlbert, O. M. Smedstad, G. R. Halliwell, P. J. Hogan, A. J. Wallcraft, R. Baraille, and R. Bleck (2007), The HYCOM (HYbrid Coordinate Ocean Model) data assimilative system, *J. Mar. Syst.*, *65*, 60–83.

Chavez, F., and T. Takahashi (2007), Coastal oceans, in *The First State of the Carbon Cycle Report (SOCCR): North American Carbon Budget and Implications for the Global Carbon Cycle*, edited by A. W. King et al., pp. 83–92, NOAA, Silver Spring, Md.

Chen, M., D. Pollard, and E. J. Barron (2003), Comparison of future climate change over North America simulated by two regional models, *J. Geophys. Res.*, *108*(D12), 4348, doi:10.1029/2002JD002738.

Colman, R. A., S. B. Power, and B. J. McAvaney (1997), Non-linear climate feedback analysis in an atmospheric general circulation model, *Clim. Dyn.*, *13*, 717–731, doi:10.1007/s003820050193.

Conkright, M. E., Locarnini R. A., Garcia H. E., O'Brien T. D., Boyer T. P., C. Stephens, and J. I. Antonov (2002), World Ocean Atlas 2001: Objective analyses, data statistics and figures CD-ROM documentation, National Oceanographic Data Center Internal Rep., 17, 17 pp., U.S. Dept. Commer., Silver Spring, Md.

DeGrandpre, M. D., G. J. Olbu, C. M. Beatty, and T. R. Hammar (2002), Air-sea CO_2 fluxes on the US Middle Atlantic Bight, *Deep Sea Res., Part II*, *49*, 4355–4367, doi:10.1016/S0967-0645(02)00122-4.

Dinniman, M. S., J. M. Klinck, and W. O. Smith Jr. (2003), Cross shelf exchange in a model of the Ross Sea circulation and biogeochemistry, *Deep Sea Res., Part II*, *50*, 3103–3120.

Druon, J. N., A. Mannino, S. Signorini, C. McClain, M. Friedrichs, J. Wilkin, and K. Fennel (2010), Modeling the dynamics and export of dissolved organic matter in the Northeastern U.S. continental shelf, *Estuarine Coastal Shelf Sci.*, *88*, 488–507.

Egbert, G. D., and S. Y. Erofeeva (2002), Efficient inverse modeling of barotropic ocean tides, *J. Atmos. Oceanic Technol.*, *19*, 183–204.

Fairall, C. W., E. F. Bradley, J. E. Hare, A. A. Grachev, and J. Edson (2003), Bulk parameterization of air-sea fluxes: Updates and verification for the COARE algorithm, *J. Clim.*, *16*, 571–591.

Feng, Y., M. A. M. Friedrichs, J. Wilkin, H. Tian, Q. Yang, E. E. Hofmann, J. D. Wiggert, and R. R. Hood (2015), Chesapeake Bay nitrogen fluxes derived from a land-estuarine ocean biogeochemical modeling system: Model description, evaluation and nitrogen budgets, *J. Geophys. Res. Biogeosci.*, *120*, 1666–1695, doi:10.1002/2015JG002931.

Fennel, K. (2010), The role of continental shelves in nitrogen and carbon cycling: Northwestern North Atlantic case study, *Ocean Sci.*, *6*, 539–548.

Fennel, K., and J. Wilkin (2009), Quantifying biological carbon export for the northwest North Atlantic continental shelves, *Geophys. Res. Lett.*, *36*, L18605, doi:10.1029/2009GL039818.

Fennel, K., J. Wilkin, J. Levin, J. Moisan, J. O'Reilly, and D. Haidvogel (2006), Nitrogen cycling in the Mid Atlantic Bight and implications for the North Atlantic nitrogen budget: Results from a three-dimensional model, *Global Biogeochem. Cycles*, *20*, GB3007, doi:10.1029/2005GB002456.

Fennel, K., J. Wilkin, M. Previdi, and R. Najjar (2008), Denitrification effects on air-sea CO_2 flux in the coastal ocean: Simulations for the Northwest North Atlantic, *Geophys. Res. Lett.*, *35*, L24608, doi:10.1029/2008GL036147.

Flather, R. A. (1976), A tidal model of the northwest European continental shelf, *Mem. Soc. R. Sci. Liege*, *6*, 141–164.

Geyer, W. R., R. P. Signell, D. A. Fong, J. Wang, D. M. Anderson, and B. A. Keafer (2004), The freshwater transport and dynamics of the western Maine coastal current, *Cont. Shelf Res.*, *24*(12), 1339–1357.

Gruber, N., P. Friedlingstein, C. B. Field, R. Valentini, M. Heimann, J. E. Richey, P. Romero Lankao, E. D. Schultze, and C.-T. A. Chen (2004), The vulnerability of the carbon cycle in the 21st century: An asssessment of carbon-climate-human interactions, in *The Global Carbon Cycle: Integrating Humans, Climate, and the Natural World*, *SCOPE*, vol. 62, edited by C. B. Field and M. R. Raupach, pp. 45–76, Island Press, Washington, D. C.

Herrmann, M., R. G. Najjar, W. M. Kemp, R. B. Alexander, E. W. Boyer, W.-J. Cai, P. C. Griffith, K. D. Kroeger, S. L. McCallister, and R. A. Smith (2015), Net ecosystem production and organic carbon balance of U.S. East Coast estuaries: A synthesis approach, *Global Biogeochem. Cycles*, *29*, 96–111, doi:10.1002/2013GB004736.

Ho, D. T., R. Wanninkhof, P. Schlosser, D. S. Ullman, D. Hebert, and K. F. Sullivan (2011), Toward a universal relationship between wind speed and gas exchange: Gas transfer velocities measured with $^3He/SF_6$ during the Southern Ocean Gas Exchange Experiment, *J. Geophys. Res.*, *116*, C00F04, doi:10.1029/2010JC006854.

Hofmann, E. E., et al. (2011), Continental shelf carbon budgets, pathways and forcing functions, *Annu. Rev. Mar. Sci.*, *3*, 93–122.

Hofmann, E., et al. (2008), Eastern U.S. continental shelf carbon budget: Integrating models, data assimilation, and analysis, *Oceanography*, *21*(1), 32–50.

Hopkinson, C. S. (1985), Shallow-water and pelagic metabolism: Evidence of heterotrophy in the near-shore Georgia Bight, *Mar. Biol.*, *87*, 19–32.

Houghton, R. W., R. Schlitz, R. C. Beardsley, B. Butman, and J. L. Chamberlin (1982), Middle Atlantic cold pool: Evolution of the temperature structure during summer 1979, *J. Phys. Oceanogr.*, *12*, 1019–1029.

Howarth, R. W., D. P. Swaney, T. J. Butler, and R. Marino (2000), Climatic control on eutrophication of the Hudson River estuary, *Ecosystems*, *3*, 210–215.

Jiang, L.-Q., W.-J. Cai, R. Wanninkhof, Y. Wang, and H. Lüger (2008), Air-sea CO_2 fluxes on the U.S. South Atlantic Bight: Spatial and seasonal variability, *J. Geophys. Res.*, *113*, C07019, doi:10.1029/2007JC004366.

Laruelle, G. G., R. Lauerwald, B. Pfeil, and P. Regnier (2014), Regionalized global budget of the CO_2 exchange at the air-water interface in continental shelf sea, *Global Biogeochem. Cycles*, *28*, 1199–1214, doi:10.1002/2014GB004832.

Laruelle, G. G., R. Lauerwalf, J. Rotschi, P. A. Raymond, J. Hartmann, and P. Regnier (2015), Seasonal response of air-water CO_2 exchange along the land-ocean aquatic continuum of the northeast North American coast, *Biogeosciences*, *12*, 1447–1458, doi:10.5194/bg-12-1447-2015.

Le Quéré, C., et al. (2009), Trends in the sources and sinks of carbon dioxide, *Nat. Geosci.*, *2*, 831–836, doi:10.1038/ngeo689.

Le Quéré, C., T. Takahashi, E. T. Buitenhuis, C. Rödenbeck, and S. C. Sutherland (2010), Impact of climate change and variability on the global oceanic sink of CO_2, *Global Biogeochem. Cycles*, *24*, GB4007, doi:10.1029/2009GB003599.

Lebo, M. E., and J. H. Sharp (1993), Phosphorus distributions along the Delaware: An urbanized coastal plain estuary, *Estuaries*, *16*, 291–302.

Lee, K., R. Wanninkhof, R. A. Feely, F. J. Millero, and T. H. Peng (2000), Global relationships of total inorganic carbon with temperature and nitrate in surface seawater, *Global Biogeochem. Cycles*, *14*, 979–94.

Lentz, S., K. Shearman, S. Anderson, A. Plueddemann, and J. Edson (2003), The evolution of stratification over the New England shelf during the Coastal Mixing and Optics study, August 1996–June 1997, *J. Geophys. Res.*, *108*(C1), 3008, doi:10.1029/2001JC001121.

Loder, J. W., and A. van der Baaren (2013), Climate change projections for the Northwest Atlantic from six CMIP5 Earth system models, *Can. Tech. Rep. Hydrogr. Ocean. Sci.* 286: xiv + 112 p.

Lutjeharms, J. R. E., P. Penven, and C. Roy (2003), Modelling the shear edge eddies of the southern Agulhas Current, *Cont. Shelf Res.*, *23*, 1099–1115.

Manning, J. P., D. J. McGillicuddy Jr., N. R. Pettigrew, J. H. Churchill, and L. S. Incze (2009), Drifter observations of the Gulf of Maine coastal current, *Cont. Shelf Res.*, *29*, 835–845.

Marchesiello, P., J. C. McWilliams, and A. F. Shchepetkin (2003), Equilibrium structure and dynamics of the California current system, *J. Phys. Oceanogr.*, *33*(4), 753–783.
Mellor, G. L., and T. Yamada (1982), Development of a turbulence closure model for geophysical fluid problems, *Rev. Geophys. Space Phys.*, *20*, 851–875.
Menzel, D. W. (1993), *Ocean Processes: U.S. Southeast Continental Shelf*, 112 pp., U.S. Dep. of Energy, Washington, D. C.
Mesinger, F., et al. (2006), North American Regional Reanalysis, *Bull. Am. Meteorol. Soc.*, *87*, 343–360.
Millero, F. J., K. Lee, and M. Roche (1998), Distribution of alkalinity in the surface waters of the major oceans, *Mar. Chem.*, *60*, 111–130.
Mountain, D. (2003), Variability in the properties of shelf water in the Middle Atlantic Bight, 1977–1999, *J. Geophys. Res. 108*(C1), 3014, doi:10.1029/2001JC001044.
Nightingale, P. D., P. S. Liss, and P. Schlosser (2000a), Measurements of air-sea gas transfer during an open ocean algal bloom, *Geophys. Res. Lett.*, *27*(14), 2117–2120, doi:10.1029/2000GL011541.
Nightingale, P. D., G. Malin, C. S. Law, A. J. Watson, P. S. Liss, M. I. Liddicoat, J. Boutin, and R. C. Upstill-Goddard (2000b), In situ evaluation of air-sea gas exchange parameterizations using novel conservative and volatile tracers, *Global Biogeochem. Cycles*, *14*(1), 373–387, doi:10.1029/1999GB900091.
O'Reilly, J. E., and D. A. Busch (1984), Phytoplankton primary production on the northwestern Atlantic shelf, *Rapp. P.-V. Reun. Cons. Int. Explor. Mer.*, *183*, 255–268.
O'Reilly, J. E., C. Evans-Zetlin, and D. A. Busch (1987), Primary production, in *Georges Bank*, edited by R. H. Backus, pp. 220–233, MIT Press, Cambridge, Mass.
Peliz, Á., J. Dubert, D. B. Haidvogel, and B. Le Cann (2003), Generation and unstable evolution of a density-driven eastern poleward current: The Iberian poleward current, *J. Geophys. Res.*, *108*(C8), 3268, doi:10.1029/2002JC001443.
Pettigrew, N. R., J. H. Churchill, C. D. Janzen, L. J. Magnum, R. P. Signesll, A. C. Thomas, D. W. Townsend, J. P. Wallinga, and H. Xue (2005), The kinematic and hydrographic structure of the Gulf of Maine coastal current, *Deep Sea Res., Part II*, *52*, 2369–2391.
Previdi, M., K. Fennel, J. Wilkin, and D. Haidvogel (2009), Interannual variability in atmospheric CO_2 uptake on the northeast U.S. continental shelf, *J. Geophys. Res.*, *114*, G04003, doi:10.1029/2008JG000881.
Pringle, J. M. (2006), Sources of variability in Gulf of Maine circulation, *Deep Sea Res., Part II*, *53*, 2457–2476.
Rhein, M., et al. (2013), Observations: Ocean, in *Climate Change 2013: The Physical Science Basis. Contribution of Working Group I to the Fifth Assessment Report of the Intergovernmental Panel on Climate Change*, edited by T. F. Stocker et al., Cambridge Univ. Press, Cambridge, U. K., and New York.
Salisbury, J. E., D. Vandemark, C. W. Hunt, J. W. Campbell, W. R. McGillis, and W. H. McDowell (2008), Seasonal observations of surface waters in two Gulf of Maine estuary-plume systems: Relationships between watershed attributes, optical measurements and surface pCO_2, *Estuarine Coastal Shelf Sci.*, *77*, 245–252.
Salisbury, J., D. Vandemark, C. Hunt, J. Campbell, B. Jonsson, A. Mahadevan, W. McGillis, and H. Xue (2009), Episodic riverine influence on surface DIC in the coastal Gulf of Maine, *Estuarine Coastal Shelf Sci.*, *82*, 108–118.
Schubel, J. R., and D. W. Pritchard (1986), Responses of upper Chesapeake Bay to variations in discharge of the Susquehanna River, *Estuaries*, *9*, 236–249.
Shchepetkin, A. F., and J. C. McWilliams (2005), The regional oceanic modeling system (ROMS): A split-explicit, free-surface, topography-following-coordinate oceanic model, *Ocean Modell.*, *9*(4), 347–404.
Shchepetkin, A., and J. C. McWilliams (1998), Quasi-monotone advection schemes based on explicit locally adaptive dissipation, *Mon. Weather Rev.*, *126*, 1541–1580.
Shchepetkin, A., and J. C. McWilliams (2003), A method for computing horizontal pressure gradient force in an oceanic model with a nonaligned vertical coordinate, *J. Geophys. Res.*, *108*(C3), 3090, doi:10.1029/2001JC001047.
Signorini, S. R., A. Mannino, R. G. Najjar Jr., M. A. M. Friedrichs, W.-J. Cai, J. Salisbury, Z. Aleck Wang, H. Thomas, and E. Shadwick (2013), Surface ocean pCO_2 seasonality and sea-air CO_2 flux estimates for the North American east coast, *J. Geophys. Res. Oceans*, *118*, 5439–5460, doi:10.1002/jgrc.20369.
Sweeney, C., E. Gloor, A. R. Jacobson, R. M. Key, G. McKinley, J. L. Sarmiento, and R. Wanninkhof (2007), Constraining global air-sea gas exchange for CO_2 with recent bomb ^{14}C measurements, *Global Biogeochem. Cycles*, *21*, GB2015, doi:10.1029/2006GB002784.
Takahashi, T., et al. (2009), Climatological mean and decadal change in surface ocean pCO_2, and net sea-air CO_2 flux over the global oceans, *Deep Sea Res., Part II*, *56*(8–10), 554–577.
Taylor, G. T., J. Way, and M. I. Scranton (2003), Planktonic carbon cycling and transport in surface waters of the highly urbanized Hudson River estuary, *Limnol. Oceanogr.*, *48*, 1779–1795.
Tian, H., Q. Yang, R. Najjar, W. Ren, M. A. M. Friedrichs, C. S. Hopkinson, and S. Pan (2015), Anthropogenic and climatic influences on carbon fluxes from eastern North America to the Atlantic Ocean: A process-based modeling study, *J. Geophys. Res. Biogeosci.*, *120*, 757–772, doi:10.1002/2014JG002760.
Townsend, D. W. (1991), Influences of oceanographic processes on the biological productivity of the Gulf of Maine, *Rev. Aquat. Sci.*, *5*, 211–230.
Townsend, D. W., A. C. Thomas, L. M. Mayer, M. Thomas, and J. Quinlan (2006), Oceanography of the Northwest Atlantic continental shelf, in *The Sea*, vol. 14, edited by A. R. Robinson and K. H. Brink, pp. 119–168, Harvard Univ. Press, Cambridge, Mass.
Vandemark, D., J. E. Salisbury, C. W. Hunt, S. M. Shellito, J. D. Irish, W. R. McGillis, C. L. Sabine, and S. M. Maenner (2011), Temporal and spatial dynamics of CO_2 air-sea flux in the Gulf of Maine, *J. Geophys. Res.*, *116*, C01012, doi:10.1029/2010JC006408.
Wang, Z., and W.-J. Cai (2004), Carbon dioxide degassing and inorganic carbon export from a marsh dominated estuary (the Duplin River): A marsh CO_2 pump, *Limnol. Oceanogr.*, *49*, 341–352.
Wanninkhof, R. (1992), Relationship between wind-speed and gas-exchange over the ocean, *J. Geophys. Res.*, *97*, 7373–7382, doi:10.1029/92JC00188.
Wanninkhof, R. (2014), Relationship between wind speed and gas exchange over the ocean revisited, *Limnol. Oceanogr. Methods*, *12*(6), 351–362.
Warner, J. C., C. R. Sherwood, H. G. Arango, R. P. Signell, and B. Butman (2005), Performance of four turbulence closure models implemented using a generic length scale method, *Ocean Modell.*, *8*, 81–113.
Wetherald, R. T., and S. Manabe (1988), Cloud feedback processes in a general circulation model, *J. Atmos. Sci.*, *45*, 1397–1415.
Wilkin, J. L. (2006), The summertime heat budget and circulation of southeast New England shelf waters, *J. Phys. Oceanogr.*, *36*(11), 1997–2011.
Yoder, J. A., J. E. O'Reilly, A. H. Barnard, T. S. Moore, and C. M. Ruhsam (2001), Variability in coastal zone color scanner (CZCS) chlorophyll imagery of ocean margin waters off the US East Coast, *Cont. Shelf Res.*, *21*, 1191–1218.